Europe PMC Funders Group
Author Manuscript
Clin Cancer Res. Author manuscript; available in PMC 2012 March 01.

Published in final edited form as:
Clin Cancer Res. 2011 March 1; 17(5): 1044–1056. doi:10.1158/1078-0432.CCR-10-2241.

FKBPL and Peptide Derivatives: Novel Biological Agents That Inhibit Angiogenesis by a CD44-Dependent Mechanism

Andrea Valentine[1,#], **Martin O'Rourke**[1,#], **Anita Yakkundi**[1], **Jenny Worthington**[2], **Michelle Hookham**[1], **Roy Bicknell**[3], **Helen O. McCarthy**[1], **Keeva McClelland**[1], **Lynn McCallum**[1], **Hayder Dyer**[1], **Hayley McKeen**[1], **David Waugh**[4], **Jennifer Roberts**[5], **Joanne McGregor**[5], **Graham Cotton**[5], **Iain James**[5], **Timothy Harrison**[5], **David G. Hirst**[1], and **Tracy Robson**[1,*]

[1]School of Pharmacy, Queen's University Belfast, Belfast, BT9 7BL, UK

[2]Biomedical Sciences, University of Ulster, Coleraine, BT52 1SA, UK

[3]Cancer Research UK Angiogenesis Group, The School of Immunity and Infection, The University of Birmingham, Birmingham, B15 2TT, UK

[4]Centre for Cancer Research and Cell Biology, Queen's University Belfast, Belfast, BT9 7BL, UK

[5]Almac Discovery, 20 Seagoe Industrial Estate, Craigavon, BT63 5QD, UK.

Abstract

Purpose—Anti-angiogenic therapies can be an important adjunct to the management of many malignancies. Here we investigated a novel protein, FKBPL, and peptide derivative for their anti-angiogenic activity and mechanism of action.

Experimental Design—Recombinant FKBPL (rFKBPL) and its peptide derivative were assessed in a range of human microvascular endothelial cell (HMEC-1) assays *in vitro*. Their ability to inhibit proliferation, migration and Matrigel dependent tubule formation was determined. They were further evaluated in an *ex-vivo* rat model of neo-vascularisation and in two *in vivo* mouse models of angiogenesis; the sponge implantation and the intra-vital microscopy models. Anti-tumor efficacy was determined in two human tumor xenograft models grown in SCID mice. Finally, the dependence of peptide on CD44 was determined using a CD44 targeted siRNA approach or in cell lines of differing CD44 status.

Results—rFKBPL inhibited endothelial cell migration, tubule formation and microvessel formation *in vitro* and *in vivo*. The region responsible for FKBPL's anti-angiogenic activity was identified and a 24 amino acid peptide (AD-01) spanning this sequence was synthesised. It was potently anti-angiogenic and inhibited growth in two human tumor xenograft models (DU145 and MDA-231) when administered systemically, either on its own, or in combination with docetaxel. The anti-angiogenic activity of FKBPL and AD-01 was dependent on the cell surface receptor CD44 and signalling downstream of this receptor promoted an anti-migratory phenotype.

Conclusion—FKBPL and its peptide derivative AD-01 have potent anti-angiogenic activity. Thus, these agents offer the potential of an attractive new approach to anti-angiogenic therapy.

Keywords

FKBPL; angiogenesis; tumor growth inhibition; CD44; anti-angiogenic

[*]Corresponding author: (T.Robson@qub.ac.uk) .
[#]These authors contributed equally to the experimental work.

Europe PMC Funders Author Manuscripts
Europe PMC Funders Author Manuscripts

Europe PMC Funders Author Manuscripts

Europe PMC Funders Author Manuscripts

Introduction

Neovascularization is critical to tumor growth and metastasis (1) and this has led to the development of anti-angiogenic agents (2). The best validated include Avastin (3), Sunitinib (4), and Sorafenib (5) which target vascular endothelial growth factor (VEGF). While they have been effective in preclinical models, only modest responses were seen in the clinic (2). Nevertheless, these agents have been approved for metastatic colorectal cancer (mCRC), non-small cell lung cancer (NSCLC), advanced breast cancer, advanced renal cell carcinoma and hepatocellular carcinoma and gastrointestinal stromal tumors. Resistance and toxicity associated with these agents has also been reported (6) including evidence that these agents can drive tumor invasion (7,8). Drugs targeting other pathways, such as the RGD-mimetic $\alpha_v\beta_3$/ $\alpha_v\beta_5$ inhibitors, have also failed to produce significant clinical responses (9), with recent evidence suggesting that low (nanomolar) concentrations of these inhibitors can paradoxically stimulate tumor growth and angiogenesis (10). Thus, development of new anti-angiogenic agents targeting alternative pathways may help to improve the therapeutic responses. In this respect, inhibitors of placental growth factor (PlGF) (11) and Delta-like 4 (Dll4) (12) are showing promise in preclinical models. However, numerous other angiogenic signalling pathways exist that could also be targeted within tumors (13). For example, alternative receptors such as CD44, a cell-surface receptor for hyaluronan, has been implicated in endothelial cell functions, angiogenesis and metastasis because of its ability to regulate both tumor and endothelial cell migration (14,15). Targeting multiple angiogenic pathways with a range of drugs may therefore provide an attractive way forward.

FKBPL belongs to the family of FK506 binding proteins (FKBP) (16,17). However, it is a divergent member of this group with shared homology mostly in the C-terminal tetra trico peptide repeat (tpr) domain, important for interactions with Hsp90. FKBPL shows low homology over the peptidyl-prolyl *cis-trans* isomerase (PPI) domain, and lacks critical residues that are required for enzymatic activity (18). We have previously shown that FKBPL affects tumor radiosensitivity (16,17) and Jascur's group identified its role in stabilising p21 in association with Hsp90 (19). We have also shown that its association with Hsp90 is also critical for regulating steroid receptor signalling, in particular the glucocorticoid receptor (GR) (20) and more recently the androgen (21) and oestrogen receptors (ER) (22). The latter study suggests that FKBPL affects ER signalling and may have both prognostic and predictive power in breast cancer patients (22). Over-expression of Hsp90 can also induce neovascularisation *in vivo* (23). In addition, Hsp90 is a major regulator of the stability and activation of angiogenesis-associated molecules, while Hsp90 inhibitors have anti-angiogenic properties (24). Therefore, the interaction of FKBPL with Hsp90 underpinned an investigation into the anti-angiogenic properties of this protein.

Here we present evidence that FKBPL is an endogenous secreted anti-angiogenic protein and demonstrate that peptides based on the active region, AD-01, are potent inhibitors of angiogenesis. This region is quite distinct from that required for its intracellular role in Hsp90 complexes, suggesting that extracellular FKBPL acts independently of Hsp90, mediating its signalling through CD44, with known roles in the regulation of endothelial and tumor cell migration (14,15).

Materials and Methods

Cell culture

The immortalised human microvascular endothelial cell line (HMEC-1) was obtained from the Centre for Disease Control and Prevention, (USA) and were maintained in MCDB-131 medium (Gibco BRL) supplemented with 10% fetal calf serum (FCS) (PAA) epidermal growth factor (EGF, 10 ng/ml) (Roche) and L-glutamine (10 mM) (Gibco BRL). All other

Europe PMC Funders Author Manuscripts

Europe PMC Funders Author Manuscripts

cells were obtained from the American Type Culture Collection and were authenticated by short tandem repeat (STR) profiling carried out by the suppliers and routine testing revealed that these cells were *Mycoplasma free*. DU145 and PC3 cells were cultured in RPMI 1640 medium (Invitrogen) supplemented with 10% foetal calf serum. MDA-231 and MCF-7 cells were maintained in DMEM (Gibco BRL) supplemented with 10% FCS. All experiments were carried out at 37°C in a humidified atmosphere of 5% CO_2 / 95% O_2.

Generation of the pcDNA3.1/endostatin construct

The pBLAST hENDO XV plasmid (InVivoGen) was digested with Hpa1 (Promega) and EcoV (Invitrogen) to release the hEndo XV insert. The hEndo XV insert was then ligated directionally into the ECoRV restriction site of pcDNA3.1 (Invitrogen).

Generation and transfection of full length or truncated FKBPL constructs

The FKBPL/pcDNA mammalian expression construct was described previously (18). To construct the 7 FKBPL truncated mutant plasmid constructs stop codons were introduced at amino acid position 34, 40, 48, 58, 86, 151 or 200 by site directed mutagenesis according to manufacturer's instructions (Quikchange kit, Stratagene) and confirmed by DNA sequencing. 1 μg of each plasmid was used for transfection of HMEC-1 cells.

Preparation of recombinant FKBPL (rFKBPL)

rFKBPL was prepared commercially by Fusion Antibodies (Belfast, UK). Standard IMAC purification was followed by desalting to remove any contaminating *E.coli* proteins.

Peptide synthesis

The 24mer peptide sequence (AD-01) NH_2-QIRQQPRDPPTETLELEVSPDPAS-OH and FKBPL 1-57mer (AL-57) sequence NH_2-METPPVNTIG EKDTSQPQQE WEKNLRENLD SVIQIRQQPR DPPTETLELE VSPDPAS-OH were assembled on an ABI 433 peptide synthesizer using modified Fmoc protocols for solid-phase peptide synthesis with commercially available protected amino acids (NovaBiochem) and confirmed to be >95% pure by analytical RP-HPLC.

Cell migration assay

The *in vitro* migration assay is a modified version of an established method (25) and is described in our previous paper (26). In brief, 90% confluent HMEC-1 cells were wounded and supplemented with fresh medium containing rFKBPL, AD-01 or AL-57. Monolayers were incubated for 7 h then fixed and the extent of "wound" closure blindly assessed microscopically. Data are expressed as % of the initial wound size at time zero (T_0) or as % inhibition compared to a time matched control. Significance was determined by one way ANOVA. All numerical data are expressed as means ± s.e.m (n=3 unless otherwise stated within the figure legend).

Tubule formation assay

The *in vitro* tubule formation assay is a modified version of a method described by others (25) and was described previously by us (26). In brief, HMEC-1 were seeded at a density of 1×10^5 onto rehydrated Matrigel™. After 1 h increasing concentrations of rFKBPL, AD-01 or AL-57 were added to each well and the plate was incubated for a further 18 h. Angiogenesis was determined from the degree of endothelial cell tubule formation (polygonal structures). An independent investigator assessed each well blindly. Each data point was expressed as an average of 5 readings per well, 3 wells per treatment group, in 3 independent experiments.

Europe PMC Funders Author Manuscripts

Europe PMC Funders Author Manuscripts

Rat aortic ring assay

This method is described in our previous paper (26). In brief, male Wistar rats were euthanised and the thoracic aorta was aseptically removed and sectioned into 1 mm thick rings, then embedded into Matrigel™ on 24 well plates. Rings were incubated for 8 days following exposure to each condition, then fixed in 4% PBS buffered paraformaldehyde. Vessel development was assessed microscopically. In four fields of view (at the upper, lower, left and right position of the ring), the number of outgrowths from the ring edge into the Matrigel were counted, and their lengths recorded to the furthest growth point. Only major branching points were included. The mean and maximum vessel length or number of vessels for each treatment group was compared to time matched sham controls and the percent inhibition calculated.

Viability/proliferation assay

An MTT assay was used to measure cell viability/proliferation as described previously (26). Briefly, HMEC-1 cells were seeded (2.5×10^3) into 96 well plates and allowed to attach for 5 h. The cells were treated for 24 and 48 h. Post incubation the cells were exposed to a 5 $mg.ml^{-1}$ solution of MTT for 4 h and OD measured spectrophotometrically. Effect on proliferation was determined by comparing treated cells to vehicle treated controls.

Sponge assay model

Polyether sponges (Calligen Foam Ltd., UK) were subcutaneously implanted into C57 black mice and injected on alternate days with 10 ng fibroblast growth factor (β-FGF) alone (n=5) or β-FGF in combination with 5μg full length rFKBPL (n=5), 0.35 μg AD-01 (molar equivalent of 5μg full-length rFKBPL; n=3) or 0.11 ng AD-01 (equivalent to 10^{-9} M *in vitro;* n=3). Sponges were removed, fixed, paraffin embedded, sectioned, stained and the vessels counted. Vessels were blindly counted by 3 independent assessors using x40 magnification in 10 fields per section. The average number of vessels per field of view in each sponge was plotted. Significance was determined by one way ANOVA.

In vivo tumor growth delay assays—5×10^6 DU145/MDA-231 tumor cells were intra-dermally injected into the rear dorsum of Balb-c severe compromised immuno-deficient (SCID) mice (Harlan, UK). For the gene delivery experiments tumors were allowed to grow to a volume of 100-125 mm^3. The mice were randomly divided into the various treatment groups and each mouse received intra-tumoral injections of Lipofectamine 2000 (Invitrogen) plasmid complexes (1 μg/μl), twice weekly, for the duration of the experiment. For the two AD-01 studies, mice with established tumors (150-175 mm^3) received daily *i.p.* injections of AD-01 or PBS as a control. In the combination study, docetaxel (20 mg/kg; i.p.) was administered once every 15 days in 3 cycles. Tumors were measured every 3 days and tumor volume was calculated as: $4/3\pi r^3$ (where r = ½ GMD and $GMD=\sqrt[3]{Length \times Breadth \times Height}$). All animal experiments were carried out in accordance with the Animal (Scientific Procedures) Act 1986 and conformed to the current UKCCCR guidelines. Significance was determined by the logrank test. Kaplan Meier analysis of the data sets was applied to determine time differences to specific events, e.g. time to tumor doubling/tripling.

Histological staining of mouse organs and immunohistochemistry

Formalin fixed paraffin embedded tissues were sectioned and stained with haematoxylin and eosin or anti-FKBPL antibody (Proteintech) followed by detection by HRP-conjugated secondary antibody.

Europe PMC Funders Author Manuscripts

Europe PMC Funders Author Manuscripts

Intravital microscopy of tumor blood vessels

Viewing chambers were inserted, under general anaesthesia, under the dorsal skin of male Balb-c SCID mice (27). Fragments of DU145 tumors were placed on the microvascular bed within the surgical area and covered with a glass microslide. When tumors reached 2 ± 0.2 mm in diameter, AD-01 was delivered i.p at 0.3 mg/kg/day for 14 days, whilst control mice received PBS. Imaging using fluorescein isothiocyanate (FITC)-labelled dextran (150 kDa) was carried out on days 0, 7 and 14 after initiating treatment using epi-florescence microscopy. Intravital images (compressed Z-stacks) were analyzed by ImageJ software (NIH, USA). Number of vessel branch points or average vessel diameter (μm) at 7 and 14 days were counted from 3D images; n=5 mice per treatment group, 4 fields of view per tumor and 30 vessels per field. Significance was determined by the two-tailed T -test.

Immunoprecipitations

To detect FKBPL in conditioned medium, agarose G-FKBPL antibody conjugate or prewashed beads (negative control) were incubated with cell lysates/pre-filtered medium according to our previously described methods (20,22). The beads were then reconstituted in Laemmli buffer and Western blot analysis was carried out to detect interacting proteins by probing for FKBPL.

Western blot analysis

Cell lysates were heated to 90°C for 10 min. Samples were subjected to SDS-PAGE electrophoresis using the Xcell SureLock Mini-cell system (Invitrogen), transferred to nitrocellulose membranes, blocked for 1 h at room temperature in 1% milk solution and probed with monoclonal anti-CD44H antibody (R&D Systems) at dilution 1:1000; anti-FKBPL antibody (Proteintech) at dilution 1:1000; GAPDH and Actin (Sigma), Rac-1 (Millipore) and then probed with either mouse or rabbit Ig HRP-linked secondary antibody (GE Healthcare) at 1:10000. Antibody binding was detected using the SuperSignal West Pico Chemiluminescent Substrate (Pierce).

Rac assay

HMEC-1 cells were pre-treated with 1 nM AD-01 prior to serum/HA stimulation (Hyaluronan, MW 220 kDa, medical grade purity, Lifecore Biomedical Inc.). Cell lysates were collected and the Rac-GTPase assay was performed on 1 mg protein using a Rac-1 activation assay kit (Upstate) according to manufacturer's instructions.

siRNA transfections—HMEC-1 cells were grown to 80% confluence then transfected for 72 h with 1.6 nM smart pool CD44 targeted siRNA or non-targeted siRNA (Dharmacon) using Lipofectin (Invitrogen) following manufacturer's instructions. Cells were then re-plated on chamber slides and subjected to the migration assay or lysates were prepared for western blot analysis.

Statistical analyses

All numerical data are expressed as means ± s.e.m. Data sets were analysed for significance with either Student's *t* test or ANOVA unless stated otherwise.

Further details on all methods can be found in supplementary methods.

Europe PMC Funders Author Manuscripts

Europe PMC Funders Author Manuscripts

Results

Over-expression of FKBPL or exposure to exogenous recombinant FKBPL inhibits angiogenesis in vitro

FKBPL in an Hsp90 co-chaperone. Based on the previous reports highlighting that Hsp90 inhibition can induce an anti-angiogenic phenotype we studied the role of FKBPL in this process. Transient over-expression of FKBPL, by transfection of HMEC-1 cells with a FKBPL cDNA mammalian expression construct, significantly inhibited cell migration *in vitro* (Fig. 1A). This effect was not restricted to the intracellular action of FKBPL since exogenous administration of purified recombinant FKBPL (rFKBPL) protein also inhibited HMEC-1 migration in a dose-dependent manner (Fig. 1B), delaying full closure of a wounded cell monolayer by 18 h compared to controls (Supplementary Fig. S1). Furthermore, administration of rFKBPL resulted in dose-dependent inhibition of HMEC-1 tubule formation on Matrigel (Fig. 1C). rFKBPL was also a potent, dose-dependent inhibitor of blood vessel development (Fig. 1D) in an *ex-vivo* rat aortic ring angiogenesis assay (26) and was 500-fold more potent than another protein-based anti-angiogenic, endostatin (28), in the same assay. Proliferation was unaffected even after exposure to the highest concentrations of rFKBPL (Supplementary Fig. S2A).

FKBPL inhibits angiogenesis in vivo in a model of neovascularisation, and inhibits the growth of DU145 human tumor xenografts

The anti-angiogenic activity of rFKBPL was further measured in subcutaneously implanted sponges *in vivo*. Treatment with 10 ng β-FGF stimulated extensive cellular in-growth into the sponges (Fig. 2A). In contrast, β-FGF-induced cellular in-growth was inhibited by co-exposure with rFKBPL (5 μg), forming significantly fewer microvessels than those treated with β-FGF alone ($p=0.032$, Fig. 2A).

Inhibition of tumor angiogenesis and tumor growth by FKBPL was compared with that of endostatin, by over-expressing these genes by direct intratumoral injection of the respective expression constructs into DU145 xenografts. Twice weekly injection of FKBPL cDNA lead to an increase in tumor FKBPL levels (Fig. 2B) and caused dramatic inhibition of tumor growth, which persisted for over 3 months (Fig. 2C); injection of the endostatin construct gave similar growth inhibition. Kaplan-Meier curves were used to measure the animals' tumor response and employed time to tumor tripling as the time that specific event. The data demonstrated significant increases in time to tripling following delivery of FKBPL or endostatin (Fig. 2D). A frequent consequence of FKBPL treatment was the development of extensive central necrosis within the tumor, which healed to reveal an empty, clean core surrounded by a viable tumor rim (Supplementary Fig. S3). This is reminiscent of the cavitation reported in clinical trials of angiogenesis inhibitors (29).

A 24 mer peptide (AD-01) spanning the N-terminal domain of FKBPL is a potent inhibitor of angiogenesis in vitro and in vivo

To elucidate FKBPL's active anti-angiogenic domain truncated FKBPL mutants were generated by site-directed mutagenesis, inserting a stop codon immediately downstream of the codons encoding aa34, aa40, aa48, aa58, aa86, aa151 and aa200 of the FKBPL cDNA (See Supplementary Fig. S4 for sequences). In the simple wound scrape assay, anti-migratory activity was retained following transient transfection of the Δ58 mutant, but lost using the Δ34 and Δ40 mutants (Fig. 3A), suggesting that the anti-migratory activity of FKBPL must reside between aa34 and aa58. Two synthetic peptides were made, one consisting of amino acids 1-57 of the FKBPL protein (i.e. the peptide encoded by the Δ58 mutant) and a 24 amino acid peptide spanning the active domain of FKBPL (i.e. amino acids 34-57; Supplementary Fig. S4). Their activity was evaluated in the HMEC-1 migration and

Europe PMC Funders Author Manuscripts

Europe PMC Funders Author Manuscripts

tubule formation assays. The FKBPL 24mer (AD-01) and 57mer (AL-57) were highly potent, with activity in the sub-nanomolar range in both of these assays (Fig. 3B; Table 1 supplementary data). However, AD-01 was superior to AL-57 in the *ex vivo* rat aortic ring assay (Fig. 3C; Table 1 supplementary data). A biphasic dose response was observed for both of these peptides similar to the rFKBPL dose response (Fig. 1B). This is consistent with studies of other drugs that target the endothelium; no specific mechanism has been clarified (30). Like rFKBPL, AD-01 did not affect endothelial cell proliferation, even at the highest doses when compared to a time matched untreated control at time points up to 48 h. (Supplementary Fig. S2B).

Having demonstrated that AD-01 had superior potency in terms of inhibiting vessel outgrowth from rat aortic rings *ex vivo*, we assessed the persistence of AD-01's effect on endothelial cell sprouting to help establish the mechanism of the anti-angiogenic effect. Vessels were allowed to develop for seven days and the medium removed and re-supplemented with medium that contained 10^{-9} M AD-01. The addition of AD-01 caused complete inhibition of vessel development when compared to time matched controls (Supplementary Fig. S5A). In contrast, aortic rings exposed to AD-01 for 7 days showed minimal sprouting, removal of drug supplemented medium and replenishment with complete medium resulted in the resumption of vessel outgrowth (Supplementary Fig. S5B). These experiments suggest that AD-01 is angiostatic and can control both immature and mature vessel outgrowth.

The anti-angiogenic activity of AD-01 was also evaluated *in vivo* using the subcutaneous murine sponge assay as previously described. AD-01 inhibited blood vessel development at both a low (p=0.0380) and high dose (p=0.0303) similar to rFKBPL (Fig. 3D).

Systemic delivery of AD-01 suppresses DU145 human tumor xenograft growth and inhibits blood vessel development in DU145 tumors

To further validate our novel peptide, AD-01 was administered daily by intra-peritoneal injection to SCID mice bearing intradermal DU145 prostate tumors. While the volume of control tumors quadrupled within 40 days, the volume of those receiving AD-01 (≥0.003 mg/kg/day) were significantly lower after 2 months treatment than at the start of treatment (Fig. 4A); suggestive of partial remission. Kaplan Meier plots revealed significantly prolonged tumor response with doses of 0.3 mg/kg (p=0.0367) and 0.003 mg/kg (p=0.0042) (Fig. 4A). To determine the efficacy of the peptide in a second tumor model, female mice were implanted intradermally with the aggressive MDA-231 breast xenograft model. Again our peptide exhibited significantly prolonged time to tripling in the experiment; as determined by Kaplan-Meier analysis, in animals treated with 0.003 mg/kg/day (p=0.0415) and 0.3 mg/kg/day (p=0.0093) (Fig. 4B). No adverse toxicity was observed during the course of the experiment and the weights of animals were stable over the treatment period (Supplementary Fig. S6). Central necrosis and cavitation of the majority of treated tumors was again observed at 60 days.

Intravital microscopy was used to assess intra-tumoral blood vessel development in DU145 tumors, implanted in the dorsal skin flap of mice (27). Blood vessels were imaged following i.v. injection of FITC–dextran on days 0, 7 and 14 after treatment with AD-01 (0.3 mg/kg/day *i.p.*), using epi-florescence microscopy (Fig. 4C). Tumor blood vessels of AD-01 treated animals demonstrated a lack of perfusion and the number of vessels was clearly reduced compared to controls; this was more obvious at the lower magnification where the whole tumor mass was imaged. Several parameters were used to quantify these differences including vessel diameter and the number of branch points (indicative of vessel number). A decrease in vessel number was observed in AD-01 treated mice compared to controls within 7 days (Fig. 4C). There was also an increase in the diameter of vessels in AD-01 treated

Europe PMC Funders Author Manuscripts

Europe PMC Funders Author Manuscripts

animals at 7 and 14 days, indicating vessel normalisation (Fig. 4C). Importantly, in contrast to the marked effect of AD-01 on tumor blood vessel number and integrity, there was no effect on the normal vasculature; retinal vasculature of animals treated with 0.3mg/kg daily i.p. for 14 days was identical to controls (Supplementary Fig. S7).

Systemic delivery of AD-01 in combination with docetaxel

The combination of Avastin® with cytotoxic chemotherapy is a promising approach to increasing cure rates (2). AD-01 was therefore combined with an established clinical regime of docetaxel, as there is evidence of improved efficacy when the Avastin was combined with docetaxel (31). The combination of docetaxel with either high or low doses of AD-01 maintained the tumors in a state of stable disease for a period of 80 days. This was most apparent in the early stages, compared to single agent (Fig. 5A). Tumors in the AD-01 alone group grew more slowly than controls, but reached a size comparable with the combination group at around 60 days due to the 'cavitation' phenomenon observed previously. Animals receiving docetaxel as a single agent were controlled until treatment ended and then re-grew rapidly with a tumor growth delay of 30 days compared to controls. The combined modality significantly enhanced time to doubling in these animals (Fig. 5B) compared with either agent alone, probably due to the enhanced control of tumor growth in the early stages. At the end of the experiment organs were removed and processed, with no difference in histology detected between liver, spleen and lung tissues excised from control or AD-01 (0.3 mg/kg/day) alone treated animals; tumors from AD-01 treated animals showed signs of significant necrosis (Fig. 5C).

FKBPL is a naturally secreted anti-angiogenic and is dependent on CD44 for its anti-angiogenic/anti-migratory activity

Although an extracellular role for FKBPL has not yet been described, we do see similar anti-angiogenic activity irrespective of whether FKBPL is endogenously over-expressed or cells are treated exogenously with rFKBPL or AD-01. It is unlikely that exogenous rFKBPL or AD-01 are passively internalised, so we sought to determine whether or not endogenously expressed FKBPL is naturally secreted. FKBPL protein was detected in the tissue culture medium of two normal cell lines, HMEC-1 and lung epithelial cells (L132), following immunoprecipitation with an anti-FKBPL antibody (Fig. 6A), however, we were unable to detect FKBPL in the medium of MDA-231 breast tumor cells unless FKBPL was stably over-expressed (Fig. 6A). This was despite similar endogenous levels of FKBPL in normal and tumor cell lines (Supplementary Fig. S8). This is consistent with anti-angiogenic responses/secretion being down-regulated in tumor cells to allow full growth potential. In order to identify a possible binding partner, we carried out bioinformatic analysis of the 24 amino acid sequence that conferred anti-angiogenic activity. This region lies outside the domain that is necessary for FKBPL's interaction with Hsp90 (i.e. FKBPL's tpr domain) so an alternative target was sought. BLAST analysis identified homology between the 24mer and a region within CD74 (Supplementary Fig. S9), known to be important for its dimerisation with CD44 (32). CD44's role in metastasis and angiogenesis has already been clearly described (14,15,33,34). We therefore investigated the role played by the cell surface hyaluronan receptor, CD44, in the FKBPL-mediated inhibition of angiogenesis. Transfection of CD44 siRNA alone did not affect HMEC-1 migration compared to controls, however, knock-down of CD44 abrogated the AD-01-mediated inhibition of HMEC-1 migration, suggesting a dependency on CD44 (Fig. 6B). In addition, both AD-01 and rFKBPL inhibited the migration of a panel of tumor cell lines in a CD44-dependent manner (Fig 6C, Supplementary Fig S10). CD44 is a cell-surface receptor that mediates migratory processes through activation of the small GTPase, Rac (34). We demonstrated activation of Rac 15 min after serum stimulation or 10 min after stimulation with CD44's natural ligand hyaluronan (HA), and this was inhibited by a 10 or 60 min pre-exposure to AD-01 (Fig 6D),

suggesting that the observed inhibition of cell migration is a consequence of AD-01-mediated inhibition of CD44/ Rac activation.

Discussion

VEGF is an established anti-angiogenic target, however, an array of side effects is now emerging in clinical practice, emphasising that VEGF and its receptors are not specific for endothelial cells (35,36). Furthermore, VEGF inhibitors can promote metastasis (7,8) and activate EPO receptors on tumor cells, which may counteract the benefits of VEGF inhibition (37). Thus, there is a need for new anti-angiogenics, targeting pathways not regulated by VEGF.

We have identified a potent, naturally secreted anti-angiogenic protein, FKBPL, which mediates its activity through CD44. Although there are some data to suggest that FKBPL is an intracellular protein associated with Hsp90 chaperone complexes (16,17, 19-22), an extracellular role has not previously been described. We now show that FKBPL is secreted. FKBPL does not contain a N-terminal signal peptide, but many cytoplasmic proteins are exported in response to specific stimuli by non-classical, ER/golgi independent protein release, regulating cell adhesion/motility upon export (38-40). These include FGF1, Ku, RHAMM, epimorphin and GAL3 amongst others (41). We have identified a new anti-angiogenic protein that is secreted to control angiogenesis. This is supported by our data showing that FKBPL can be detected in the medium of “normal” cells, but cannot be detected in the medium of tumor cells except when artificially over-expressed. This hypothesis may explain our recent demonstration that high FKBPL mRNA levels are prognostic for improved overall survival and distant metastasis-free survival in a cohort of untreated breast cancer patients (22), consistent with an anti-angiogenic role for this protein. However, this would need to be further clarified.

The anti-angiogenic activity of FKBPL resides within a 24 aa domain; this is outside the domain required for an interaction with Hsp90 (i.e. the tpr domain) suggesting that Hsp90 is not responsible for either the chaperoning of FKBPL to the extracellular milieu, nor for subsequent anti-angiogenic signalling. We have now demonstrated that FKBPL mediates its activity through the CD44 pathway. Although the exact mechanisms are yet to be fully elucidated, AD-01 inhibits endothelial cell migration (and this is dependent on high levels of CD44; Fig. 6B and C), tubule formation and angiogenesis in several *ex vivo* and *in vivo* models, while having no effect on the proliferative capacity of endothelial cells. This differentiates AD-01 from the other approved VEGF-targeted agents and is important, given that major adverse effects of anti-angiogenic drugs are associated with their broad spectrum of anti-proliferative activity (6).

The complexity of CD44 signalling has made its role in angiogenesis and metastasis difficult to elucidate. The presence of splice variant forms of CD44 have been associated with tumor progression whilst other studies on the standard form (CD44s) suggest an association with decreased metastasis and enhanced survival (42,43). CD44 knockdown has been shown to inhibit angiogenesis (15), though treatment of mice with KM81, a bioactive anti-murine CD44 antibody (which blocks HA binding), failed to inhibit the neovascularization of matrigel implants (44). Furthermore, CD44-null mice are viable with no obvious morphological defects, which suggests possible compensation by other receptors such as RHAMM (45). Our own data suggest that AD-01 signals through CD44, inhibiting the Rho GTPase, Rac, a well-known regulator of actin assembly and activator of migration (Fig 6D). Further studies will be required to appreciate the full role of CD44 in the AD-01 mediated inhibition of cell migration.

Europe PMC Funders Author Manuscripts
Europe PMC Funders Author Manuscripts

Europe PMC Funders Author Manuscripts

Europe PMC Funders Author Manuscripts

We have demonstrated that AD-01 is a highly potent anti-angiogenic agent across a range of models *in vitro*. It was more potent that the larger peptide, AL-57, in the rat aortic ring assay which may be due to a lack of penetration of the larger peptide into this *ex vivo* tissue. Furthermore, AD-01 had no effect on proliferation, nor is it cytotoxic. *In vivo* it was effective against two tumor xenograft models, prostate and breast. Its combination with docetaxel achieved complete control, particularly in the early stages compared to AD-01 alone, which would be very favourable clinically. Nevertheless, tumors treated with AD-01 alone were equally well-controlled at 60 days suggesting that it could also be useful as a single agent. It would be useful in future combination studies to assess re-growth of these tumors after ceasing treatment; whilst we would expect re-growth to occur (supported by data in Supplementary Fig. S5B), we might also be able to demonstrate more effective cell killing in the combination group compared to AD-01 alone. The *in vivo* tumor growth delay data (Figs 4 and 5) also demonstrate that our targeting approach must be dependent on CD44 expression within the tumor vasculature and not the tumor parenchyma, since DU145 cells do not express CD44 at detectable levels. This is supported by the window chamber data (Fig. 4 C), which demonstrate that the vasculature in the DU145 xenograft model is severely compromised within 7 days of AD-01 treatment. Thus, AD-01 has broad applicability across a wide range of solid tumors whether or not they express CD44.

In summary, this is the first description of a role for FKBPL as an anti-angiogenic protein. Its peptide derivative, AD-01, holds promise as an anti-angiogenic for cancer therapy and could have potential when resistance to and/or escape from existing VEGF therapies has developed.

Translational Relevance

Anti-angiogenic therapies targeting VEGF/VEGFR2 have recently been approved for clinical use in certain types of cancer. However, these drugs have not produced enduring efficacy, suggesting evasive resistance and highlighting the need for new agents targeting an alternative pathway. These could be used either in combination with the current inhibitors or in tumors developing resistance to such agents. We now show that a novel protein, FKBPL, and peptide derivatives based on the active anti-angiogenic domain of this protein function as direct inhibitors of angiogenesis, affecting pathways that control endothelial cell motility by signalling through CD44. These peptides are currently undergoing preclinical evaluation and may provide the first-in-class peptide-based therapies for targeting tumor angiogenesis by an entirely different pathway to those agents currently approved.

Supplementary Material

Refer to Web version on PubMed Central for supplementary material.

Acknowledgments

We wish to thank the staff of the Biological Services Units at QUB for their assistance with *in vivo* experiments, and the staff of the Histopathology Unit at CCRCB for the preparation of tissue sections.

Financial support: Almac Discovery and Action Cancer, Northern Ireland.

REFERENCES

1. Bergers G, Benjamin LE. Tumorigenesis and the angiogenic switch. Nat Rev Cancer. 2003; 3:401–10. [PubMed: 12778130]

Europe PMC Funders Author Manuscripts

2. Jain RK, Duda DG, Clark JW, Loeffler JS. Lessons from phase III clinical trials on anti-VEGF therapy for cancer. Nat Clin Pract Oncol. 2006; 3:24–40. [PubMed: 16407877]
3. Ferrara N, Hillan KJ, Gerber HP, Novotny W. Discovery and development of bevacizumab, an anti-VEGF antibody for treating cancer. Nat Rev Drug Discov. 2004; 3:391–400. [PubMed: 15136787]
4. Motzer RJ, Bukowski RM. Targeted therapy for metastatic renal cell carcinoma. J Clin Oncol. 2006; 24:5601–8. [PubMed: 17158546]
5. Wilhelm S, Carter C, Lynch M, et al. Discovery and development of sorafenib: a multikinase inhibitor for treating cancer. Nat Rev Drug Discov. 2006; 5:835–44. [PubMed: 17016424]
6. Verheul HM, Pinedo HM. Possible molecular mechanisms involved in the toxicity of angiogenesis inhibition. Nat Rev Cancer. 2007; 7:475–85. [PubMed: 17522716]
7. Ebos JM, Lee CR, Cruz-Munoz W, et al. Accelerated metastasis after short-term treatment with a potent inhibitor of tumor angiogenesis. Cancer Cell. 2009; 15:232–9. [PubMed: 19249681]
8. Pàez-Ribes M, Allen E, Hudock J, et al. Antiangiogenic therapy elicits malignant progression of tumors to increased local invasion and distant metastasis. Cancer Cell. 2009; 15:220–31. [PubMed: 19249680]
9. Reardon DA, Fink KL, Mikkelsen T, et al. Randomized Phase II Study of Cilengitide, an Integrin-Targeting Arginine-Glycine-Aspartic Acid Peptide, in Recurrent Glioblastoma Multiforme. J Clin Oncol. 2008; 26:5610–7. [PubMed: 18981465]
10. Reynolds AR, Hart IR, Watson R, et al. Stimulation of tumor growth and angiogenesis by low concentrations of RGD-mimetic integrin inhibitors. Nat Med. 2009; 15:392–400. [PubMed: 19305413]
11. Fischer C, Mazzone M, Jonckx B, Carmeliet P. FLT1 and its ligands VEGFB and PlGF: drug targets for anti-angiogenic therapy? Nat Rev Cancer. 2008; 8:942–56. [PubMed: 19029957]
12. Thurston G, Noguera-Troise I, Yancopoulo GD. The Delta paradox: DLL4 blockade leads to more tumor vessels but less tumor growth. Nat Rev Cancer. 2007; 7:327–31. [PubMed: 17457300]
13. Carmeliet P. Angiogenesis in life, disease and medicine. Nature. 2005; 438:932–6. [PubMed: 16355210]
14. Martin TA, Harrison G, Mansel RE, Jiang WG. The role of the CD44/ezrin complex in cancer metastasis. Crit Rev Oncol Hematol. 2003; 46:165–86. [PubMed: 12711360]
15. Cao G, Savani RC, Fehrenbach M, et al. Involvement of endothelial CD44 during *in vivo* angiogenesis. Am J Pathol. 2006; 169:325–36. [PubMed: 16816384]
16. Robson T, Price ME, Moore ML, et al. Increased repair and cell survival in cells treated with DIR1 antisense oligonucleotides: implications for induced radioresistance. Int J Radiat Biol. 2000; 76:617–23. [PubMed: 10866283]
17. Robson T, Joiner MC, Wilson GD, et al. A novel human stress response-related gene with a potential role in induced radioresistance. Radiat Res. 1999; 152:451–61. [PubMed: 10521921]
18. Kay JE. Structure-function relationships in the FK506-binding protein (FKBP) family of peptidylprolyl cis-trans isomerases. Biochem J. 1996; 2:361–85. [PubMed: 8670043]
19. Jascur T, Brickner H, Salles-Passador I, et al. Regulation of p21(WAF1/CIP1) stability by WISp39, a Hsp90 binding TPR protein. Mol Cell. 2005; 17:237–49. [PubMed: 15664193]
20. McKeen HD, McAlpine K, Valentine A, et al. A novel FK506-like binding protein interacts with the glucocorticoid receptor and regulates steroid receptor signaling. Endocrinology. 2008; 149:5724–5734. [PubMed: 18669603]
21. Sunnotel O, Hiripi L, Lagan K, McDaid J, et al. Alterations in the steroid hormone receptor co-chaperone FKBPL are associated with male infertility: a case-control study. Repro Biol Endocrinol. 2010; 8:22.
22. McKeen HD, Byrne C, Jithesh PV, et al. FKBPL regulates estrogen receptor signaling and determines response to endocrine therapy. Cancer Res. 2010; 7:1090–100. [PubMed: 20103631]
23. Pfosser A, Thalgott M, Büttner K, et al. Liposomal Hsp90 cDNA induces neovascularization via nitric oxide in chronic ischemia. Cardiovasc Res. 2005; 65:728–36. [PubMed: 15664400]
24. Kaur G, Belotti D, Burger AM, et al. Antiangiogenic properties of 17-(dimethylaminoethylamino)-17-demethoxygeldanamycin: an orally bioavailable heat shock protein 90 modulator. Clin Cancer Res. 2004; 10:4813–21. [PubMed: 15269157]

Europe PMC Funders Author Manuscripts

Europe PMC Funders Author Manuscripts

25. Ashton AW, Yokota R, John G, et al. Inhibition of Endothelial Cell Migration, Intercellular communication, and vascular tube formation by thromboxane A2*. J Biol Chem. 1999; 274:35562–70. [PubMed: 10585431]
26. O'Rourke M, Ward C, McKeown SR, et al. Evaluation of the anti-angiogenic potential of AQ4N. Clin Cancer Res. 2008; 14:1502–9. [PubMed: 18316575]
27. Tozer GM, Ameer-Beg SM, Baker J, et al. Intravital imaging of tumor vascular networks using multi-photon fluorescence microscopy. Adv Drug Deliv Rev. 2005; 57:135–52. [PubMed: 15518926]
28. Kruger EA, Duray PH, Tsokos MG, et al. Endostatin inhibits microvessel formation in the *ex vivo* rat aortic ring angiogenesis assay. Biochem Biophys. Res Commun. 2000; 268:183–91. [PubMed: 10652234]
29. Crabb SJ, Patsios D, Sauerbrei E, et al. Tumor cavitation: impact on objective response evaluation in trials of angiogenesis inhibitors in non-small-cell lung cancer. J Clin Oncol. 2009; 27:404–10. [PubMed: 19047292]
30. Folkman J. Angiogenesis. Annual Review of Medicine. 2006; 57:1–18.
31. Ramaswamy B, Elias AD, Kelbick NT, et al. Phase II trial of bevacizumab in combination with weekly docetaxel in metastatic breast cancer patients. Clin Cancer Res. 2006; 12:3124–9. [PubMed: 16707611]
32. Shi X, Leng L, Wang T, et al. CD44 is the signaling component of the macrophage migration inhibitory factor-CD74 receptor complex. Immunity. 2006; 25:595–606. [PubMed: 17045821]
33. Hill A, McFarlane S, Mulligan K, et al. Cortactin underpins CD44-promoted invasion and adhesion of breast cancer cells to bone marrow endothelial cells. Oncogene. 2006; 25:6079–91. [PubMed: 16652145]
34. Bourguignon LY, Zhu H, Shao L, Chen YW. CD44 interaction with tiam1 promotes Rac1 signaling and hyaluronic acid-mediated breast tumor cell migration. J Biol Chem. 2000; 275:1829–38. [PubMed: 10636882]
35. Verheul HM, Pinedo HM. Possible molecular mechanisms involved in the toxicity of angiogenesis inhibition. Nat Rev Cancer. 2007:7475–85.
36. Roodhart JM, Langenberg MH, Witteveen E, Voest EE. The molecular basis of class side effects due to treatment with inhibitors of the VEGF/VEGFR pathway. Curr Clin Pharmacol. 2008; 3:132–43. [PubMed: 18690886]
37. Tam BY, Wei K, Rudge JS, et al. VEGF modulates erythropoiesis through regulation of adult hepatic erythropoietin synthesis. Nat Med. 2006; 12:793–800. [PubMed: 16799557]
38. Nickel W. Unconventional secretory routes: direct protein export across the plasma membrane of mammalian cells. Traffic. 2005; 6:607–614. [PubMed: 15998317]
39. Prudovsky I, Tarantini F, Landriscina M, et al. Secretion without Golgi. J Cell Biochem. 2007; 103:1327–43. [PubMed: 17786931]
40. Radisky DC, Hirai Y, Bissell MJ. Delivering the message: epimorphin and mammary epithelial morphogenesis. Trends Cell Biol. 2003; 13:426–34. [PubMed: 12888295]
41. Jeffery CJ. Moonlighting proteins. Trends Biochem Sci. 1999; 24:8–11. [PubMed: 10087914]
42. Bourguignon LY. Hyaluronan-mediated CD44 activation of RhoGTPase signaling and cytoskeleton function promotes tumor progression. Semin Cancer Biol. 2008; 18:251–9. [PubMed: 18450475]
43. Naor D, Wallach-Dayan SB, Zahalka MA, Sionov RV. Involvement of CD44, a molecule with a thousand faces, in cancer dissemination. Semin Cancer Biol. 2008; 18(4):260–7. [PubMed: 18467123]
44. Savani RC, Cao G, Pooler PM, et al. Differential involvement of the hyaluronan (HA) receptors CD44 and receptor for HA-mediated motility in endothelial cell function and angiogenesis. J Biol Chem. 2001; 276:36770–8. [PubMed: 11448954]
45. Teder P, Vandivier RW, Jiang D. Resolution of lung inflammation by CD44. Science. 2002; 296:155–8. [PubMed: 11935029]

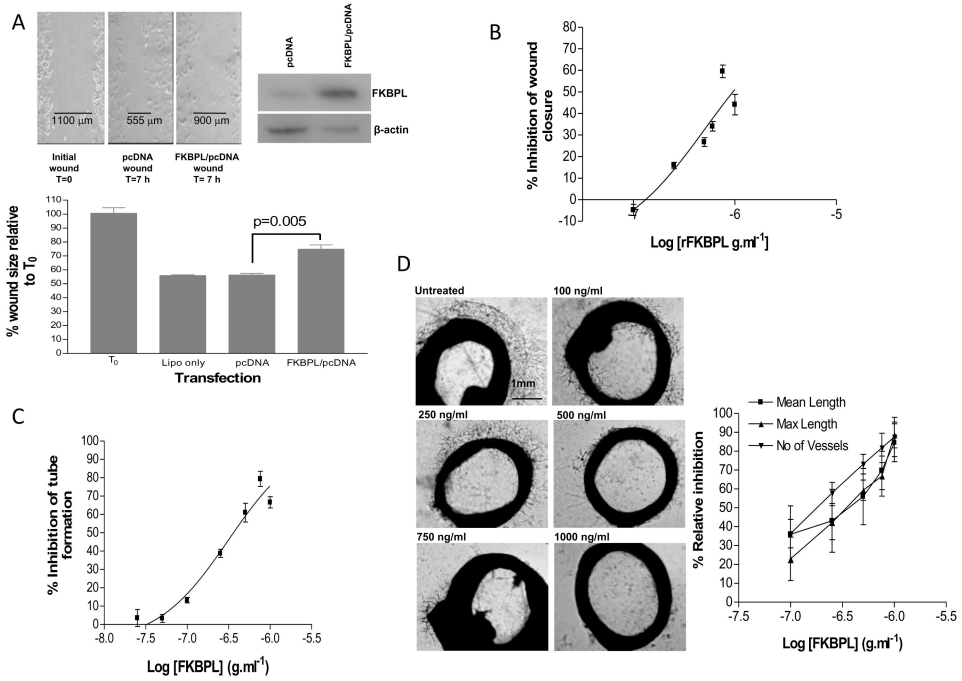

Figure 1.

rFKBPL protein inhibits angiogenesis *in vitro* and *ex vivo* **(A)** Transient transfection of an FKBPL cDNA construct inhibits migration of wounded HMEC-1 monolayers compared to empty vector controls. Representative images of wounded monolayers and overexpression of FKBPL following transfection. The histogram shows the wound size relative to wound size at time=0 h ± SEM; n=3. Significance was determined by ANOVA. **(B)** Inhibition of HMEC-1 wound closure (compared to time matched control) after exposure to a range of concentrations of rFKBPL. Data points show means ± SEM; n=3. **(C)** Inhibition of HMEC-1 tubule formation in matrigel following exposure to increasing concentrations of rFKBPL; data are corrected to a sham treated control. Data points are means ± SEM; n=3. **(D)** Microvessel sprouting from rat aortic rings incubated with increasing concentrations of rFKBPL (left panel). Quantitative determination of vessel length and number of vessels after 7 days compared to time matched controls (right panel). Data points are means ± SEM; n=3.

Europe PMC Funders Author Manuscripts
Europe PMC Funders Author Manuscripts

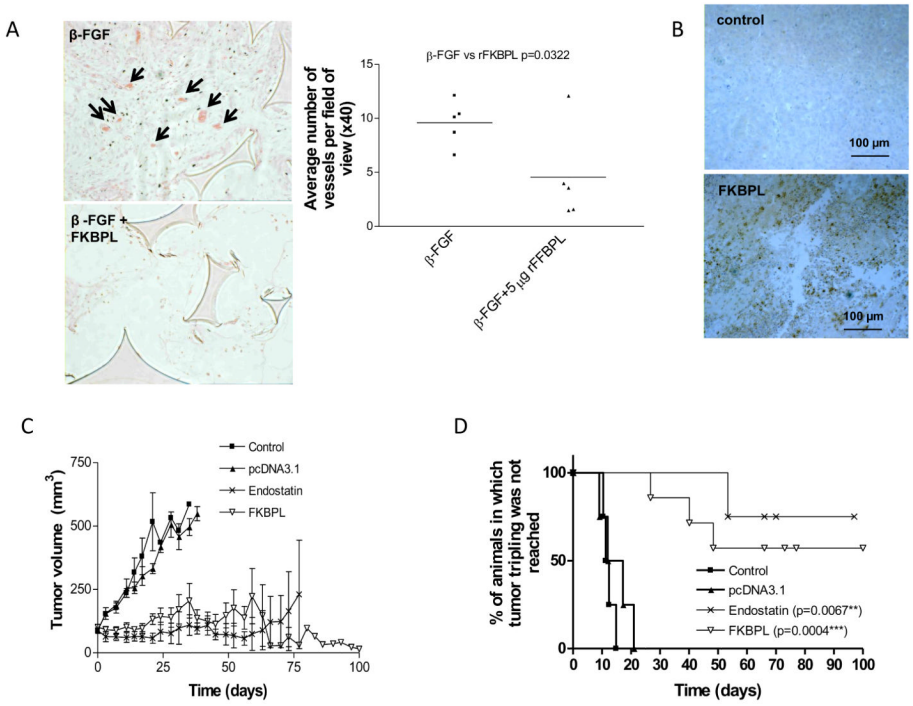

Figure 2.

FKBPL inhibits angiogenesis *in vivo* and prevents the growth of DU145 human tumor xenografts **(A)** rFKBPL (5 ng injected directly into the sponge on alternate days) inhibited β-FGF (10 ng)-induced angiogenesis in C57 black mice. 14 days after implant there was a marked decrease in vessel density and cellular ingrowth in rFKBPL-treated sponges (left panel; representative image-arrows indicate vessels containing bright eosin stained erythrocytes). Graph shows quantification of microvessel density in β-FGF alone or β-FGF +rFKBPL-injected sponges. Each symbol represents the average number of vessels per x40 field, with 10 fields counted blindly in 5 sponges. n=5 mice/sponges per treatment group. **(B)** Immunohistochemistry showing FKBPL expression in DU145 tumors grown in SCID mice after injection with a cDNA construct expressing FKBPL. **(C)** DU145 tumors grown in SCID mice were intra-tumorally injected twice weekly for the duration of the experiment with 25 μg of a cDNA construct expressing either FKBPL or endostatin (as a positive control), or pcDNA3.1 empty vector (as a negative control). Graph shows tumor volume over time ± SEM; n=4-7 mice per condition. **(D)** Kaplan Meier survival curves; *significance was determined by the Logrank test.

Europe PMC Funders Author Manuscripts
Europe PMC Funders Author Manuscripts

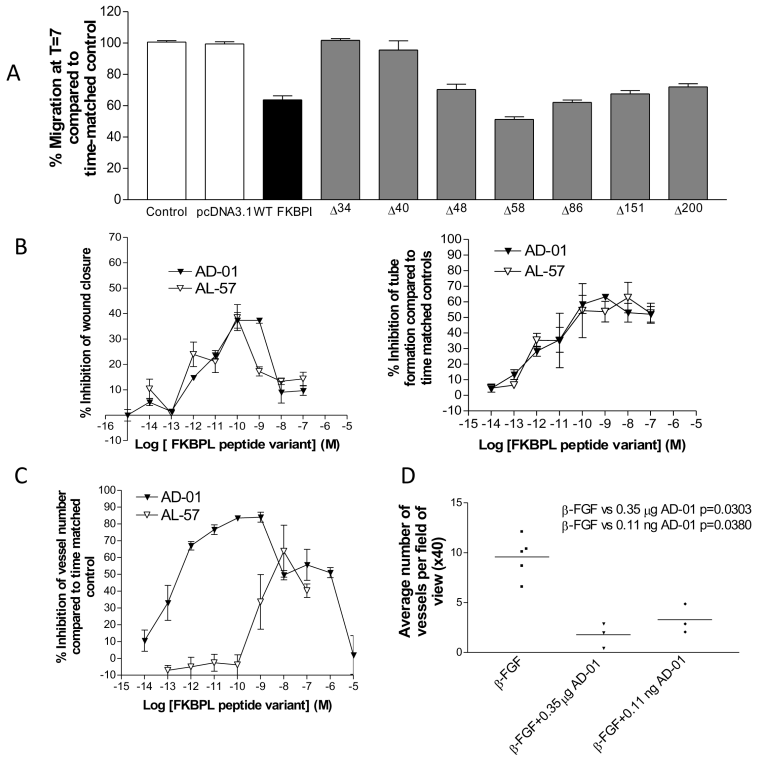

Figure 3.

The active domain within FKBPL resides between aa-34-58 and a 24mer-based peptide, AD-01, spanning this domain inhibits angiogenesis and is more potent than rFKBPL. **(A)** Wound size of HMEC-1 monolayers 7 h after transfection with truncated DNA constructs; n=3. **(B)** Inhibition of migration (left panel; compared to time matched controls) and tubule formation (right pane; compared to time matched controlsl) of HMEC-1 cells after treatment with AD-01/AL-57 peptides across a range of concentrations. Data points are means ± SEM; n=3. **(C)** Inhibition of microvessel sprouting from rat aortic rings (compared to time matched controls ± SEM) incubated for 7 d with a range of concentrations of AD-01/AL-57; n=3. **(D)** AD-01 inhibited β-FGF-induced angiogenesis in the sponge assay *in vivo*. Microvessel densities in implanted sponges treated with in β-FGF alone (10 ng) or or β-FGF + AD-01 (0.35 μg or 0.11 ng). Each symbol represents the average number of vessels per x40 field, with 10 fields counted blindly in each sponge; n= 5 mice/sponges for β-FGF alone; n=3 mice/sponges for AD-01 treatment.

Europe PMC Funders Author Manuscripts
Europe PMC Funders Author Manuscripts

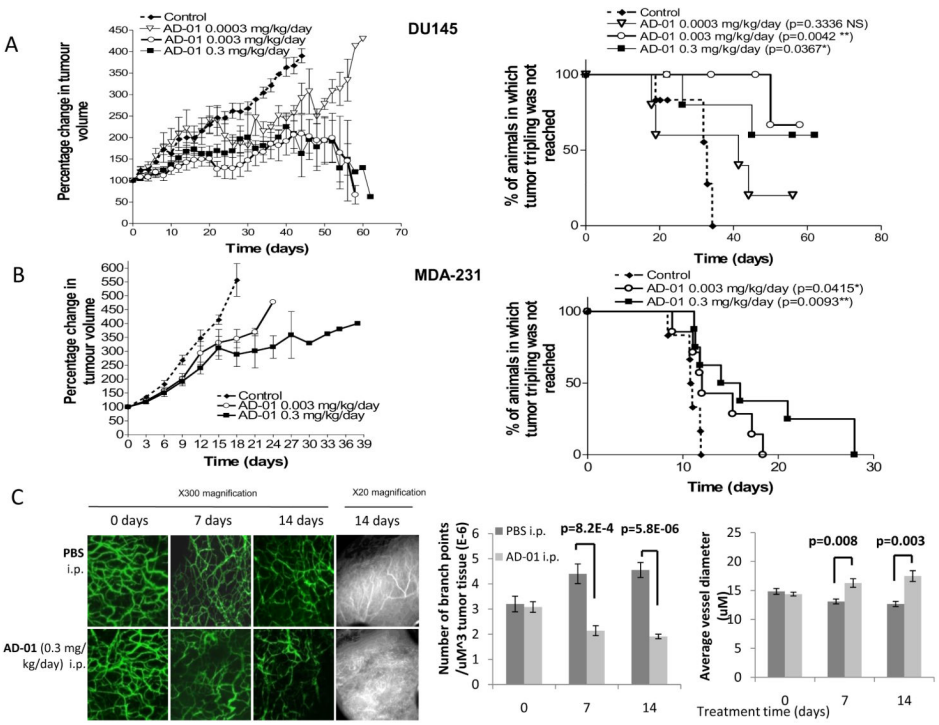

Figure 4.

Systemic delivery of AD-01 inhibits blood vessel development and tumor growth **(A)** Growth curves for DU145 xenografts or MDA-231 **(B)** with or without daily i.p injection of a range of doses of AD-01. Data points are means ±SEM; n= 5-8 mice per treatment group and Kaplan Meier survival curves with time to tumor tripling volume as the endpoint for survival; *significance was determined by the Logrank test. **(C)** Intravital images (compressed Z-stacks) of DU145 xenografts showing blood vessels at 7 and 14 days after the start of treatment with AD-01 (0.3mg/kg/day) or PBS control, *i.p.* (left panel). Number of vessel branch points or average vessel diameter (μm) at 7 and 14 days after initiating treatment with AD-01 (0.3mg/kg/day, *i.p.*) or PBS ± SEM; n=5 mice per treatment group, 4 fields of view per tumor and 30 vessels per field. Significance was determined by the two-tailed T -test.

Europe PMC Funders Author Manuscripts
Europe PMC Funders Author Manuscripts

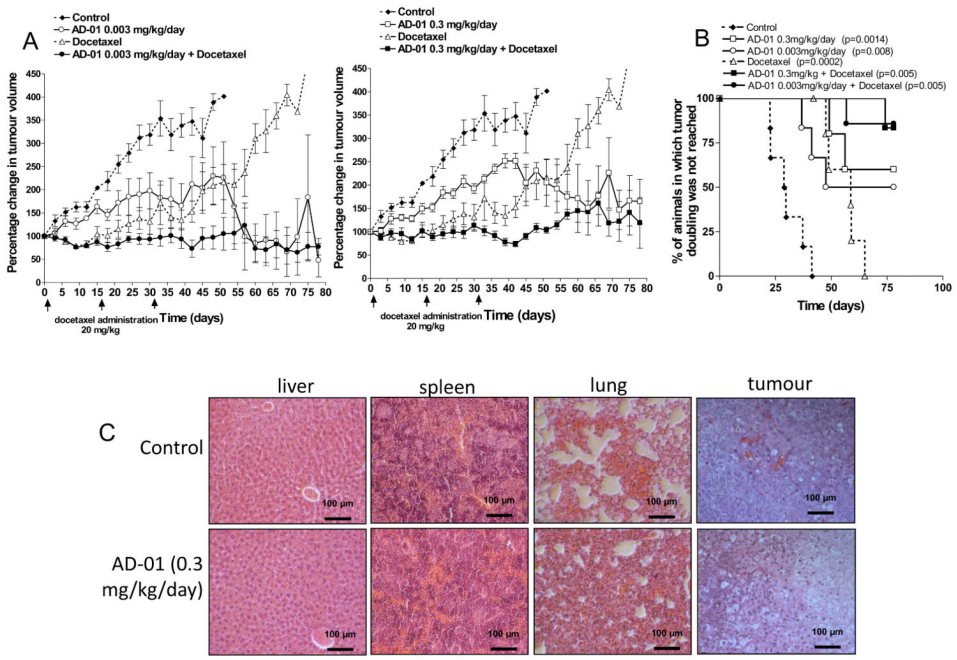

Figure 5.

Systemic delivery of AD-01 inhibits DU145 tumor growth in combination with docetaxel. **(A)** Fold change in tumor volume following treatment with AD-01 (0.3 and 0.003 mg/kg/d, i.p.) in combination with docetaxel (20 mg/kg once every 15 days in 3 cycles) compared to PBS alone, AD-01 alone and docetaxel alone controls ± SEM; n= 5-7 mice per treatment group. **(B)** Kaplan Meier survival curves with time to tumor doubling as the endpoint for survival. *significance was determined by the Logrank test. **(C)** Haematoxylin and eosin staining of FFPE tissue sections taken from control animals and animals exposed to high dose AD-01 (0.3 mg/kg/day) at the end of the experiment; no obvious toxicity was observed.

Europe PMC Funders Author Manuscripts
Europe PMC Funders Author Manuscripts

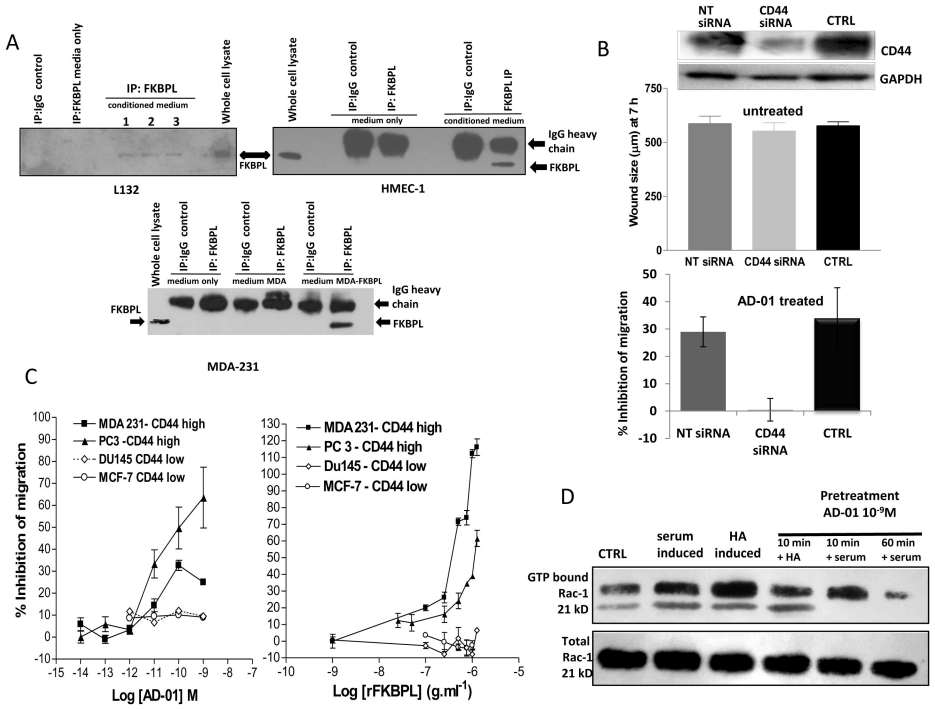

Figure 6.

FKBPL is secreted and is dependent on CD44 for its anti-angiogenic activity **(A)** IP western blots using conditioned medium from HMEC-1, L132 and MDA-231 cells 24 h after plating. FKBPL was IPed using an anti-FKBPL antibody and then run on a western blot and probed for FKBPL. Control medium (no cell exposure) or immunoprecipitation with an IgG control were used as negative controls. Whole cell lystates were used as positive controls. **(B)** Inhibition of migration of HMEC-1 compared to time matched control 72 h after transfection with non-targeted siRNA compared to CD44 targeted siRNA in untreated cells (upper graph) and treated (10^{-9}M AD-01; lower graph) ± SEM; n=5. **(C)** Migration of tumor cells after treatment with AD-01 (left panel) or rFKBPL (right panel) across a range of concentrations (± SEM; n=3). **(D)** Representative gel showing inhibition of rac activity in HMEC-1 cells after treatment with AD-01 (10^{-9}M) for 10 min/60 min prior to serum/HA activation.

Europe PMC Funders Author Manuscripts
Europe PMC Funders Author Manuscripts